

# Synthesizing Non-Uniformly Excited Antenna Arrays Using Tiled Subarray Blocks

Jafar Ramadhan Mohammed

Ninevah University, Mosul, Iraq

<https://doi.org/10.26636/jtit.2023.4.1417>

**Abstract** — Conventionally, non-uniformly excited antenna arrays are synthesized by independently determining the excitation amplitude and phase of each single element. Such an approach is considered to be the most expensive and complex design method available. In this paper, the tiling technique is harnessed to synthesize non-uniformly excited antenna arrays. To apply this technique, the array elements are first divided into different sub-array shapes, such as rectangles or squares known as tiles. The use of rectangular tile blocks instead of a single element architecture greatly simplifies the array design process and reduces array complexity. Next, the problem concerned with synthesizing sub-arrays comprising rectangular tile blocks is formulated and solved by using horizontal and vertical orientations of tiles having different shapes and sizes, and their larger integer expansions. The third approach to tiled design is a mixture of both previous tile architectures. A genetic algorithm is used to design such tiled arrays offering optimum sidelobe levels, beam width, directivity and taper efficiency. Simulation results demonstrated the effectiveness of the proposed tiled arrays.

**Keywords** — antenna arrays, non-uniform amplitudes, performance optimization, tiled subarray blocks

## 1. Introduction

Antenna arrays are capable of providing many desired radiation characteristics, such as beam forming, beam scanning, pattern reconfiguration and high directive gains for current and future wireless communication systems. Large antenna arrays composed of many radiating elements placed along rectangular grids are a solution that is best suited for achieving these desired characteristics. However, these large, fully-populated arrays that consist of a single transmit/receive module for each element of the planar array are generally complex and expensive. Thus, they are unattractive for many applications, especially for use in satellites, where low-profile antennas with low costs are needed [1]–[2]. The addition of adaptive multi-beamforming capabilities to these arrays will increase their implementation costs even further.

To solve these problems, different subarray configurations have been proposed in the last years. In [3]–[4], the authors proposed sparse arrays, whereas in [5]–[9], thinned arrays were suggested as a method capable of effectively reducing the number of transmit/receive modules in the array feeding network. Generally, thinned arrays are associated with direc-

tivity degradation, due to the fact that several array elements are turned off. Thus, clustered arrays [10]–[13] or partially adaptive arrays [14]–[15] are more preferable due to their ability to provide high directive gains.

On the other hand, the tiling technique is a promising strategy in reducing array complexity. The authors in [16] proposed an optimum algorithm to generate tile structures, while the authors in [12] used the tiling technique to synthesize aperiodic tiling planar antenna arrays. The works described in [17]–[18], which are related to the optimized design of tiled arrays, have proved the effectiveness of the tiling technique in synthesizing antenna arrays. Recently, these tiling techniques are continuously gaining in popularity due to their simplified feeding network requirements, as the array elements are divided into different regular or irregular tiles and each tile is equipped with a single transmit/receive module, thus increasing array modularity, which leads to a significant reduction in the implementation cost. Although irregular tiles are more complex than their regular counterparts, they are the preferred solution due to the absence of undesired grating lobes in their radiation patterns. However, the problem of un-tilability, i.e., the lack of ability to divide the entire array aperture into tiles, may exist in irregular tiled arrays. In such a case, determination of an optimized tiled configuration will not be an easy task, as there is a huge number of various tiling options available. This renders the method highly time consuming. In this paper, amplitude weighting of non-uniformly excited antenna arrays is first performed with the use of rectangular tile blocks with different orientations and sizes to achieve

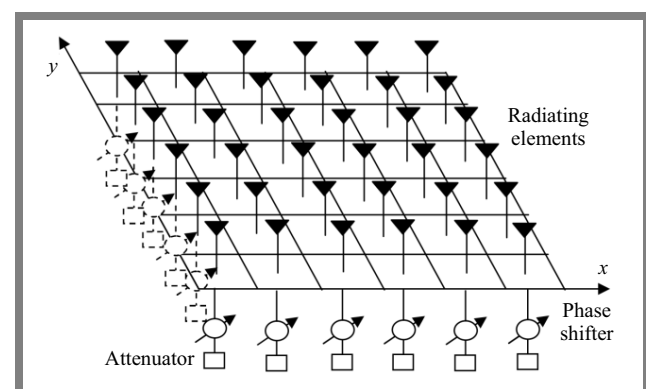
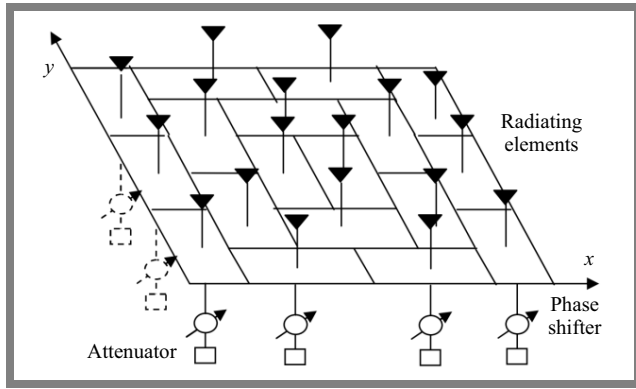


Fig. 1. Element-based architecture of a fully populated array.



**Fig. 2.** Tile architecture of the proposed array.

the irregularity property. The first design consists of an array aperture divided into small tile blocks with sizes and orientations of  $1 \times 2$  and  $2 \times 1$ . The second design considers larger tile blocks ( $2 \times 4$  and  $4 \times 2$  configurations), while the third design mixes the two tile configurations described above. A genetic algorithm is used to optimize the amplitude weights of these tiled arrays under specific user-defined constraints, resulting in improved radiation patterns, optimum sidelobe levels, specific beam widths, and improved taper efficiency.

## 2. Tiled Arrays

Consider a two-dimensional rectangular planar antenna array made up of  $E = N \times M$  elements. These elements are symmetrically distributed on the  $x - y$  plane, with uniform inter-element spacing on both  $x$  and  $y$  axes  $d = d_x = d_y$  over the entire array aperture, as shown in Fig. 1.

Assume that these elementary radiators are arranged and grouped into a set of tiles equal to  $T$  as shown in Fig. 2. These tile blocks should fully cover the array aperture. Each single tile  $t = 1, 2, \dots, T$  (where  $T$  is the total number of tiles) is assumed to be composed of a number of sub-elementary radiators equal to  $1 \times L$  for the horizontal orientation scenario,  $L \times 1$  for the vertical orientation scenario, or equal to their multiple integer expansions  $t = i(1 \times L)$  and  $t = i(L \times 1)$  where  $i$  is an integer number that control the sizes of the tiles. When  $i \geq 2$ , larger tiles may be obtained and, consequently, a higher degree of modularity is achieved that helps further reduce the required number of transmit/receive modules,

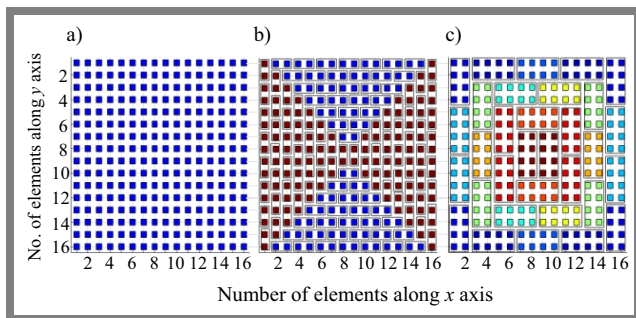


**Fig. 3.** Array layouts: a) conventional element-based array without tiles, b) tiled array with  $1 \times 2$  and  $2 \times 1$  tiles, and c) tiled array with  $2 \times 4$  and  $4 \times 2$  tiles.

thus resulting in a simplified array feeding network. The optimization problem consists in finding the optimal number and positions of the horizontal and vertical tiles that precisely cover the entire array aperture, in accordance with specific user-defined constraints affecting the resulting tiled array pattern. Generally, array radiation patterns may be expressed as [19]:

$$AP(\theta, \varphi)_{dB} = 10 \log [EP(\theta, \varphi) \times AF(\theta, \varphi)] , \quad (1)$$

where  $EP(\theta, \varphi)$  is the elementary pattern which is considered to be  $EP(\theta, \varphi) = \cos^{1.2}(\theta, \varphi)$  and  $AF(\theta, \varphi)$  is the array factor given by:

$$AP(\theta, \varphi) = \sum_{e=1}^E a_e e^{j\rho_e} e^{jk(x_e \sin \theta \cos \varphi + y_e \sin \theta \cos \varphi)} , \quad (2)$$

where  $E$  is the total number of array elements,  $a_e$  and  $\rho_e$  are the amplitudes and phases of the elementary array weights,  $x_e$  and  $y_e$  are the element locations on the  $x$  and  $y$  axis, respectively,  $k = 2\pi/\lambda$ ,  $\lambda$  is the wavelength in the free space, while  $\theta$  and  $\varphi$  are the elevation and azimuth angles. The horizontal and vertical rectangular tiles,  $t = i(1 \times L)$  and  $t = i(L \times 1)$  are formed by grouping each  $i \times L$  adjacent sub-elementary radiators with a single tiled weight. The tiled amplitude weights vector can be written as:

$$w = \sum_{t=1}^T A \delta_{c_e}^t \quad e = 1, 2, \dots, E , \quad (3)$$

where  $T$  is the total number of tiles,  $E$  is the total number of array elements,  $A$  and  $\delta_{c_e}^t$  are the tiled amplitudes and the Kronecker delta function, respectively, defined as:

$$A_t = \frac{1}{i \times L} \sum_{e=1}^E a_e \delta_{c_e}^t \quad t = 1, 2, \dots, T , \quad (4)$$

$$\delta_{c_e}^t = \begin{cases} 1 & \text{if } c_e = t \\ 0 & \text{if } c_e \neq t \end{cases} . \quad (5)$$

From Eqs. (4) and (5), it is clear that when  $\delta_{c_e}^t = 1$ , the  $e$ -th element belongs to the  $t$ -th tile. Then, each tiled amplitude weight  $A_t$  is computed by taking the average or mean value of the referenced elementary amplitude weights  $a_e$  that belong to the same tile under consideration.

For an array of  $E = N \times M = 16 \times 16$ , an integer number of  $i = 1$ , and a number of sub-elements in each of  $L = 2$ , a  $1 \times 2$  tile block is formed in the horizontal orientation scenario and a  $2 \times 1$  tile block is created in the vertical orientation case, as shown in Fig. 3b. The total number of tile blocks is 128. The sizes of the tile blocks become  $2 \times 4$  and  $4 \times 2$  for  $i = 2$  and the total number of the tiles equals 32, as shown in Fig. 3c. The total number of potential tiling solutions capable of completely covering the entire array aperture amounts to, for the two above-mentioned cases, approximately  $8 \times 10^{19}$  and  $1 \times 10^8$ , respectively.

For larger arrays, the number of potential options will increase rapidly. Thus, deployment of the optimization algorithm to identify all the potential options and determine the best tile configuration that guarantees the coverage of the entire array aperture is time consuming.

The proposed optimization solution aims at using a pre-specified block configuration shown in Fig. 3b-c in order to meet specific user-defined constraints concerning the resulting tiled array patterns and guaranteeing complete coverage of the entire array aperture. Thus, the problem of time consumption may be solved and, at the same time, performance of the tiled array can be maintained (remaining as equal as possible to the optimal value). This can be achieved by introducing the following cost function:

$$\text{Cost} = \sum_{s=1}^S \left| AF(\theta_s, \varphi_s) - \text{Constraints}(\theta_s, \varphi_s) \right|^2, \quad (6)$$

where  $S$  is the total number of the sample points used for evaluating the difference between the obtained and the optimal array pattern described by the specific constraints. The constraints in terms of the desired sidelobe level (SLL) and beam width (BW) may be defined as:

$$\text{Constraints} = \begin{cases} SLL, -1 \leq 0 \leq -\frac{2}{BW}, \frac{2}{BW} \leq 0 \leq 1 \\ 0, -\frac{2}{BW} \leq 0 \leq BW \end{cases}. \quad (7)$$

Note that all the values in Eq. (7) are in decibels and they are normalized to 0 dB. The optimization algorithm applied consists of the following steps:

- 1) Initialize the genetic algorithm by creating a set of initial populations and specify the total number of iterations. An initial population size equals 50, the number of marriages is 25, and number of iterations is set to 1000.
- 2) Generate the required constraints according to Eq. (7) by applying user-defined limits, such as upper sidelobe level, lower sidelobe level, and the required width of the main beam between the first null-to-null beamwidth. These constraints (see the dashed red line in Fig. 6 represent the reference pattern or the ideal pattern that needs to be achieved during the optimization process).
- 3) Generate a new set of individuals with the following specifications: roulette wheel selection, single point crossovers, mutation probability, and a mating pool. The number of crossovers is 2, the mutation probability is 0.04, and the mating pool is chosen to be 4.
- 4) For each a single individual, evaluate iteratively the cost function according to the user-defined constraints given in Eqs. (6) and (7). The number of pattern points between the obtained array pattern and the one required according to Eq. (6) is 512.
- 5) Among all the current individuals, keep the best one that corresponds to the optimized tiled weights according to Eqs. (4) and (5).
- 6) The steps starting with item 2 are repeated iteratively until the final number is reached.

### 3. Simulation Results

In this section, the proposed tiled subarray blocks are analyzed and assessed by relying on various numerical examples. In all of the examples, a square array with fully populated

elements (in the  $16 \times 16$  configuration) is considered. An optimized array of fully elementary radiators with optimal amplitude weights is considered as a reference solution. User-defined constraints concerning the desired sidelobe level and first null-to-null beam width are  $SLL = -30$  dB and  $BW = 10^\circ$ , respectively.

In the first example, a small two-cell tile block of sizes of  $1 \times 2$  and  $2 \times 1$  is validated. The layout of the fully optimized

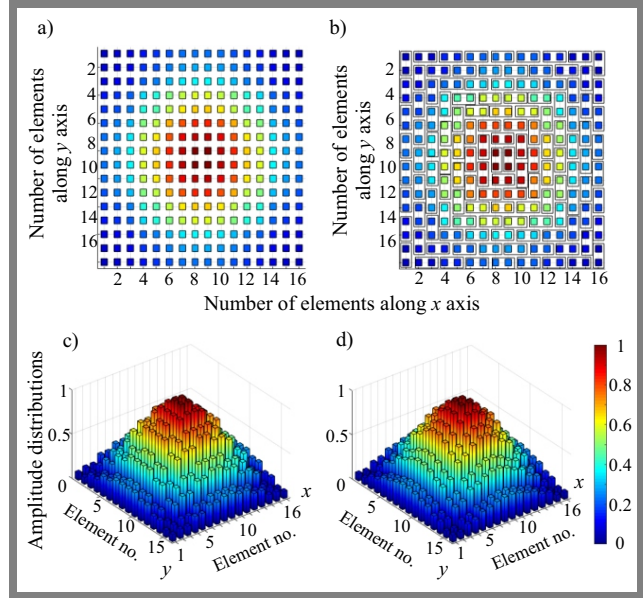


**Fig. 4.** Optimized amplitudes of element-based and tiled arrays, their layouts a)–b) and their weights for  $1 \times 2$  and  $2 \times 1$  tiles c)–d).

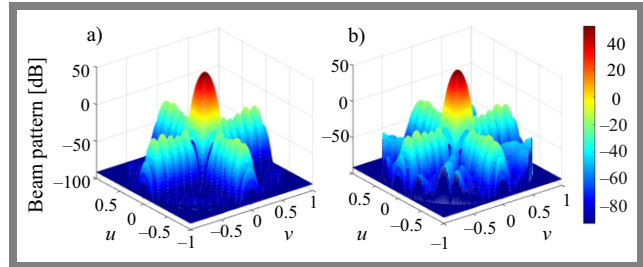


**Fig. 5.** Three-dimensional array patterns of the fully optimized element-based array a) and the proposed tiled array for  $1 \times 2$  and  $2 \times 1$  tiles b).

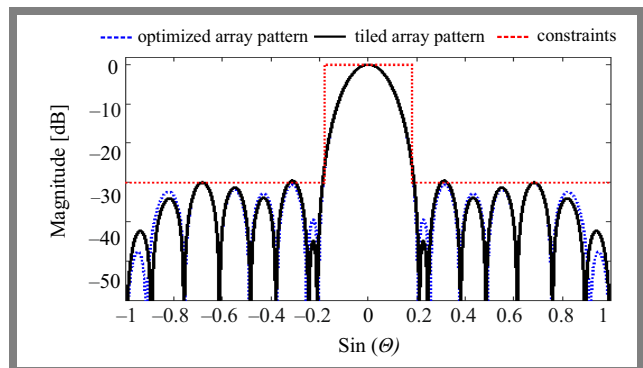


**Fig. 6.** Two-dimensional array patterns of the fully optimized element-based array and the proposed tiled array for  $1 \times 2$  and  $2 \times 1$  tiles.

array and the layout of the proposed tiled array, with optimized amplitude weights of the tiles, are shown in Fig. 4. Their corresponding three-dimensional radiation patterns are shown in Fig. 5. To compare these two-array patterns at element and tile levels, their two-dimensional radiation patterns at the cut-plane of  $u = 0$  are plotted together, as shown in Fig. 6.

From these figures, it can be concluded that the use of small tile blocks of sizes of  $1 \times 2$  and  $2 \times 1$  are effective and reliable. Its resulting tiled array pattern is optimal, since it is very close to that of the optimized, referenced solution. In addition, all the user-defined constraints are fully met where all the sidelobes are below  $-30$  dB and the first null-to-null beam width is exactly  $10^\circ$ . However, the feeding network complexity (i.e., the number of the required transmit/receive modules) is only reduced by half, since each two adjacent elements are made as a single block to which a single tile's amplitude weight is attached.

In the second example, horizontal and vertical tile blocks of sizes of  $2 \times 4$  and  $4 \times 2$  are considered to further simplify the array feeding network. The tiled layout, the optimized amplitude weights, and the corresponding two dimensional radiation patterns are shown in Fig. 7. It can be seen that the same constraints cannot met due to the availability of a smaller number of variable tiled weights. Thus, a trade-off is needed between complexity and the desired constraints.

In the next example, different tile blocks of sizes of  $1 \times 2$ ,  $2 \times 1$ ,  $2 \times 4$  and  $4 \times 2$  are considered. The results applicable to such mixed tile architectures are shown in Fig. 8, where both the complexity and the desired radiation constraints are traded off in the best possible manner.

Finally, the performance was measured in terms of taper efficiency, directivity, peak sidelobe level and average side lobe level. The total area under the sidelobe pattern and the average deviation of all sidelobe peaks that appear above the required sidelobe limit for all the above tiled arrays are reported in Tab. 1. For the first type of the design, one may observe that SLL, directivity, taper efficiency and the average SLL deviation are exactly same as those of the optimal referenced solution. For the other design, directivity and taper efficiency values are only 0.3 dB and 4% higher, respectively, than those of the optimal referenced solution. For the third scenario, all the parameters once again reached the optimal values. These results fully confirm the effectiveness of the proposed tiled array designs.

## 4. Conclusions

In this paper, an effective antenna array synthesis method based on tiled subarray blocks rather than depending on single independent elementary radiators has been described. The tiled blocks can provide designers of large antenna arrays with numerous advantages. To offer optimal performance, the configuration of the tiles and their amplitude weights were optimized by using a powerful optimization tool, such as the genetic algorithm. To reduce the time spent on searching for various options, specific rectangular tile blocks with sizes of

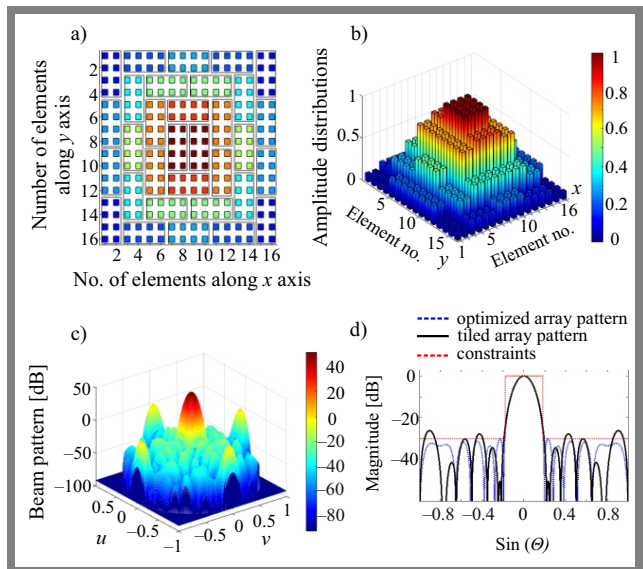


**Fig. 7.** Results for  $2 \times 4$  and  $4 \times 2$  tile configurations: a) array layout, b) optimized amplitude weights and the resulting radiation patterns of the fully optimized element-based array, and the proposed tiled array in c) 3D and d) 2D.

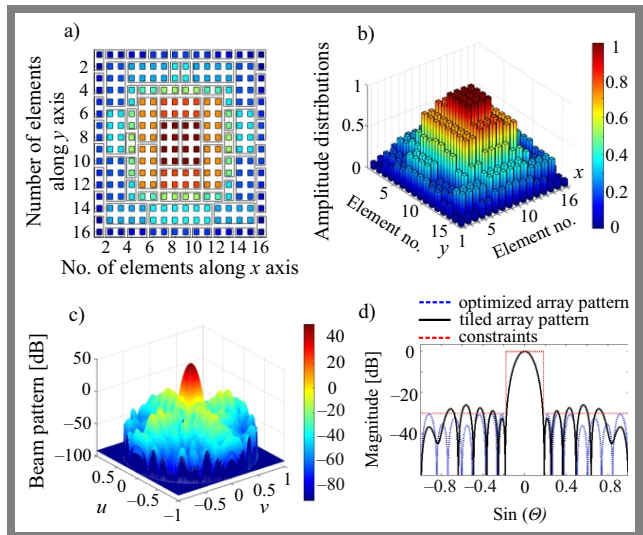


**Fig. 8.** Results for a mixed architecture of  $1 \times 2$ ,  $2 \times 1$ ,  $2 \times 4$ , and  $4 \times 2$  tiles: a) tile layout, b) amplitude weights, radiation patterns of the fully optimized element-based array and the proposed tiled array in c) 3D, and d) 2D.

$i(1 \times L)$ , and  $i(L \times 1)$  were used and genetic optimization was solely used to find the optimal values of the tile amplitude weights that meet the user-defined constraint requirements. The obtained results prove the effectiveness of the described method, showing an exact match between measured performance values and the referenced optimal solutions in the case of small tile block sizes, and identifying some deviations in the case of larger tile block sizes.

## References

- [1] J.S. Herd and M.D. Conwey, "The Evolution to Modern Phased Array Architectures", *Proceedings of the IEEE*, vol. 104, no. 3, pp. 519–529, 2016 (<https://doi.org/10.1109/JPROC.2015.2494879>).


**Tab. 1.** Performance measures for various array designs for  $N \times M = 16 \times 16$ .

Designed arrays	Number of tiles	Directivity [dB]	Taper efficiency	Peak SLL	Average SLL	Average SLL deviation
Ordinary uniform array	0	20.38	1	-13.2	-12.07	-7.0
Standard Dolph array	0	18.94	0.861	-30	-16.13	0
Fully optimized elementary array	0	18.88	0.855	-30	-16.21	0
Tiled array (design 1)	128	18.60	0.828	-30	-16.0	-0.5
Tiled array (design 2)	32	18.52	0.815	-26	-15.6	-3.5
Tiled array (design 3)	69	18.95	0.860	-26	-15.3	-2.3

- [2] R.J. Mailloux, *Phased Array Antenna Handbook*, 2nd ed., Norwood: Artech House, 2005 (ISBN: 9781580536899).
- [3] M.A. Abdelhay, N.O. Korany, and S.E. El-Khamy, "Synthesis of Uniformly Weighted Sparse Concentric Ring Arrays Based on Off-Grid Compressive Sensing Framework", *IEEE Antennas and Wireless Propagation Letters*, vol. 20, no. 4, pp. 448–452, 2021 (<https://doi.org/10.1109/LAWP.2021.3052174>).
- [4] J.R. Mohammed, R. Hamdan, and A.J. Abdulqader, "Linear and Planar Array Pattern Nulling via Compressed Sensing", *Journal of Telecommunications and Information Technology*, vol. 3, pp. 50–55, 2021 (<https://doi.org/10.26636/jtit.2021.152921>).
- [5] J.R. Mohammed, "A Method for Thinning Useless Elements in the Planar Antenna Arrays", *Progress in Electromagnetics Research Letters*, vol. 97, pp. 105–113, 2021 (<https://doi.org/10.2528/PIERL21022104>).
- [6] M. Salucci, G. Gottardi, N. Anselmi, and G. Oliveri, "Planar Thinned Array Design by Hybrid Analytical-stochastic Optimization", *IET Microwaves, Antennas and Propagation*, vol. 11, no. 13, pp. 1841–1845, 2017 (<https://doi.org/10.1049/iet-map.2017.0349>).
- [7] J.R. Mohammed, "Thinning a Subset of Selected Elements for Null Steering Using Binary Genetic Algorithm", *Progress in Electromagnetics Research M*, vol. 67, pp. 147–157, 2018 (<https://doi.org/10.2528/PIERM18021604>).
- [8] W.P.M.N. Keizer, "Linear Array Thinning Using Iterative FFT Techniques", *IEEE Transactions on Antennas and Propagation*, vol. 56, no. 8, pp. 2757–2760, 2008 (<https://doi.org/10.1109/TAP.2008.927580>).
- [9] R.L. Haupt, "Thinned arrays using genetic algorithms", *IEEE Transactions on Antennas and Propagation*, vol. 42, no. 7, pp. 993–999, 1994 (<https://doi.org/10.1109/8.299602>).
- [10] J.R. Mohammed, "Minimization of Grating Lobes in Large Arrays Using Clustered Amplitude Tapers", *Progress in Electromagnetics Research C*, vol. 120, pp. 93–103, 2022 (<https://doi.org/10.2528/PIERC22031706>).
- [11] P. Rocca, G. Oliveri, R.J. Mailloux, and A. Massa, "Unconventional Phased Array Architectures and Design Methodologies – A Review", *Proceedings of the IEEE*, vol. 104, no. 3, pp. 544–560, 2016 (<https://doi.org/10.1109/JPROC.2015.2512389>).
- [12] V. Pierro, V. Galdi, G. Castaldi, I.M. Pinto, and L.B. Felsen, "Radiation Properties of Planar Antenna Arrays Based on Certain Categories of Aperiodic Tilings", *IEEE Transactions on Antennas and Propagation*, vol. 53, no. 2, pp. 635–644, 2005 (<https://doi.org/10.1109/TAP.2004.841287>).
- [13] R.J. Mailloux, S.G. Santarelli, T.M. Roberts, and D. Luu, "Irregular Polyomino-shaped Subarrays for Space-based Active Arrays", *International Journal of Antennas and Propagation*, vol. 2009, art. no. 956524, 2009 (<https://doi.org/10.1155/2009/956524>).
- [14] T. Yeong *et al.*, "Shape and Weighting Optimization of a Subarray for a mm-Wave Phased Array Antenna", *Applied Sciences*, vol. 11, no. 15, art. no. 6803, 2021 (<https://doi.org/10.3390/app11156803>).
- [15] J.R. Mohammed, "Synthesizing Sum and Difference Patterns with Low Complexity Feeding Network by Sharing Element Excitations", *International Journal of Antennas and Propagation*, vol. 2017, art. no. 2563901, pp. 1–7, 2017 (<https://doi.org/10.1155/2017/2563901>).
- [16] S. Desreux and E. Remila, "An Optimal Algorithm to Generate Tilings", *Journal of Discrete Algorithms*, vol. 4, no. 1, pp. 168–180, 2006 (<https://doi.org/10.1016/j.jda.2005.01.003>).
- [17] A.J. Abdulqader, J.R. Mohammed, and Y.A. Ali, "A T-Shaped Polyomino Subarray Design Method for Controlling Sidelobe Level", *Progress in Electromagnetics Research C*, vol. 126, pp. 243–251, 2022 (<https://doi.org/10.2528/PIERC22080803>).
- [18] P. Rocca, N. Anselmi, A. Polo, and A. Massa, "An Irregular Two-sizes Square Tiling Method for the Design of Isophoric Phased Arrays", *International Journal of Antennas and Propagation*, vol. 68, no. 6, pp. 4437–4449, 2020 (<https://doi.org/10.1109/TAP.2020.2970088>).
- [19] J.R. Mohammed, "Rectangular Grid Antennas with Various Boundary Square-Rings Array", *Progress in Electromagnetics Research Letters*, vol. 96, pp. 27–36, 2021 (<https://doi.org/10.2528/PIERL20112402>).

**Jafar Ramadhan Mohammed, Prof.**

College of Electronic Engineering

 <https://orcid.org/0000-0002-8278-6013>

E-mail: [jafar.mohammed@uoninevah.edu.iq](mailto:jafar.mohammed@uoninevah.edu.iq)

Ninevah University, Mosul, Iraq

<https://uoninevah.edu.iq>